Available online at www.sciencedirect.com
ScienceDirect
Journal of Organometallic Chemistry 692 (2007) 4661–4668
Journal of Organometallic Chemistry
www.elsevier.com/locate/jorganchem

Ion pair symmetrization in metallocenium cations partnered with diborane derived borate counteranions

Lee D. Henderson, Warren E. Piers *

Department of Chemistry, University of Calgary, 2500 University Drive NW, Calgary, Alberta, Canada T2N 1N4

Received 30 March 2007; received in revised form 14 May 2007; accepted 14 May 2007
Available online 24 May 2007

Dedicated with great respect to Prof. Gerhard Erker, a hero of metallocene chemistry.

Abstract

The thermodynamics of ion pair symmetrization in a series of metallocenium species generated from Cp''_2ZrMe_2 ($Cp'' = 1,2\text{-}Me_2C_5H_3$) were studied using a variety of solution dynamic techniques including line broadening, 2D-EXSY, and 1D-DPFGSE-NOE. Ion pairs were generated by methide abstraction using the corresponding trityl salts [**1-A**] to yield $[Cp''_2ZrMe]^+[A]^-$ ($A = \{C_6F_4\text{-}1,2\text{-}[B(C_6F_5)_2]_2\text{-}(\mu\text{-}O(C_6F_5))\}^-$, **2-O(C$_6F_5$)**; $\{C_6F_4\text{-}1,2\text{-}[B(C_6F_5)_2]_2(\mu\text{-}OPh)\}^-$, **2-OPh**; $\{C_6F_4\text{-}1,2\text{-}[B(C_6F_5)_2]_2(\mu\text{-}OMe)\}^-$, **2-OMe**; and $[B(C_6F_5)_4]^-$, **2-B(C$_6$F$_5$)$_4$**). The observed activation parameters were interpreted on the basis of a solvent-assisted mechanism of ion pair symmetrization.

Keywords: Metallocenes; Ion pair symmetrization; Weakly coordinating anions; Fluoroarylborates

1. Introduction

Metallocenium ion pairs formed from neutral dialkyl derivatives Cp_2MR_2 and an alkide abstractor are the active catalysts in olefin polymerization systems of significant industrial importance [1]. For this reason, their structural and dynamic properties have been studied extensively, since these features have direct impact on catalyst activity and selectivity [2]. A key determinant in the behavior of these catalysts is the nature of the cation–anion interaction, the strength of which is dictated by a number of integrated factors including the coordinating properties of the anion, the structure and symmetry of the cation, the steric/electronic properties of the growing polymer chain and the polarity of the solvent medium.

Deconvoluting these variables to develop a detailed understanding of the dynamic properties of these ion pairs has occupied the efforts of several groups over the past decade. Many studies have made use of NMR techniques to extract the kinetic and thermodynamic parameters of ion pair dynamics by using metallocenium or non-metallocenium cations that incorporate diastereotopic groups whose chemical exchange is observable on the NMR time scale. Pioneering studies by Marks et al. [3] utilized the group 4 tetramethyl metallocenes shown in Scheme 1 to identify two key processes in systems activated by the strong organometallic Lewis acid $B(C_6F_5)_3$ [4] and related species. In these systems, the anion partner is a relatively strongly bound methyl borate anion, $[MeB(C_6F_5)_3]^-$. As shown in the scheme, "borane dissociation/recombination" permutes not only the diastereotopic groups on the Cp rings, but also the M–Me/BMe groups, while "ion pair symmetrization" (ips) exchanges the former but not the latter. It is thus possible to observe these processes separately using this probe. Brintzinger [5] has also utilized various systems with similar symmetry properties to study these processes, while subsequently others have engaged in various studies to probe the kinetic and thermodynamic properties of

* Corresponding author.
E-mail address: wpiers@ucalgary.ca (W.E. Piers).

0022-328X/$ - see front matter © 2007 Elsevier B.V. All rights reserved.
doi:10.1016/j.jorganchem.2007.05.023

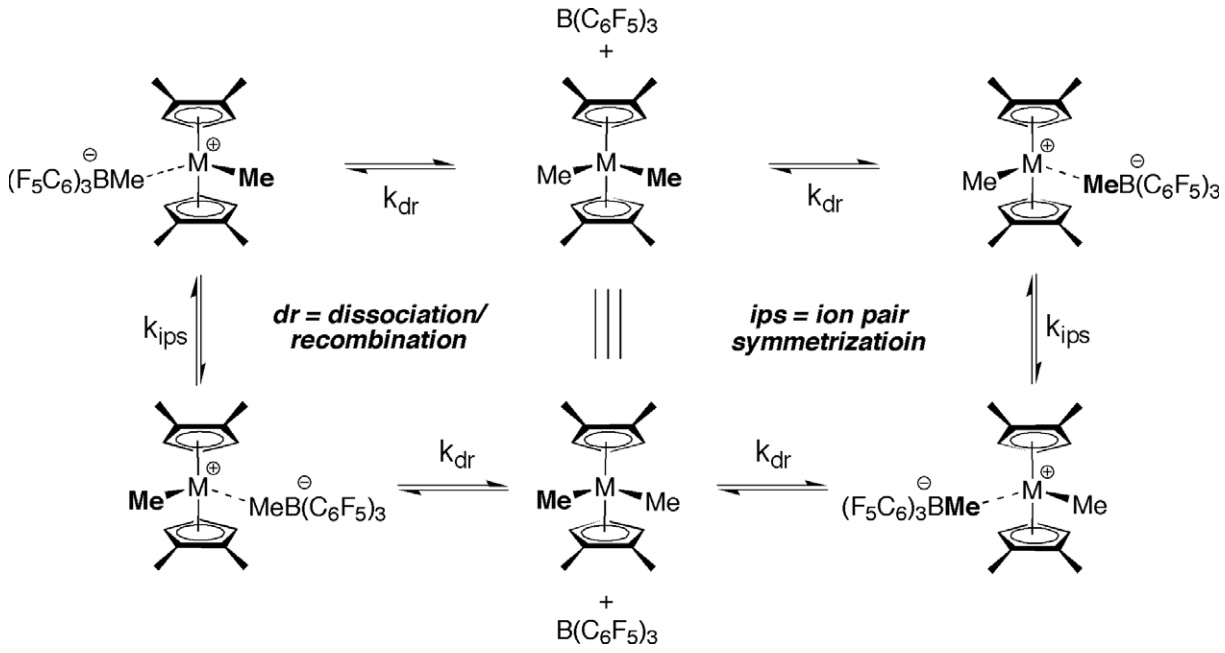

Scheme 1.

metallocenium ion pairs from both experimental [6–10] and computational [11] perspectives.

The nature of the ips process in particular has engendered extensive discussion, since activation entropies range from moderately positive to moderately negative values, depending on the structure of the metallocene, the concentration regime the experiments have been performed in, and the nature of the anion. Mechanistic postulates have therefore also spanned a range of suggestions, including those that are dissociative in character and ones that involve ion pair aggregates and are thus associative in nature. Since full dissociation of the anion is expected to be highly energetic, more recently solvent molecules have been proposed to play a significant role in the exchange process [2b,11l,11m].

The majority of above mentioned studies consider ion pairs with the more coordinating (and stabilizing) $[MeB(C_6F_5)_3]^-$ counteranion. Measurements on ion pairs containing more weakly coordinating anions such as $[B(C_6F_5)_4]^-$ have proven more difficult [2a,5c,12]. We have prepared a family of borate anions [13] based on the chelating perfluoroaryl borane C_6F_4-1,2-$[B(C_6F_5)_2]_2$ [14], that can be conveniently prepared as their trityl salts and used to activate metallocenes via methide abstraction. In this contribution, we describe ion pair symmetrization studies for a series of ion pairs generated from Cp''_2ZrMe_2 ($Cp'' = 1,2\text{-}Me_2C_5H_3$) and trityl salts of the $\{C_6F_4$-1,2-$[B(C_6F_5)_2]_2(\mu\text{-}OR)\}^-$ ($R = Me$, C_6H_5, C_6F_5) anions and the $[B(C_6F_5)_4]^-$ borate anion. Using a combination of solution dynamics techniques including coalescence determination, line broadening, 2D-EXSY, and 1D-DPFGSE-NOE we report the rate constants and activation parameters in these systems.

2. Results and discussion

All the ion pairs studied were generated by methide abstraction protocols using the $[CPh_3]^+$ cation, affording ion pairs with weakly coordinating borate counteranions and Ph_3CMe as the by-product [15]. The production of ion pairs by this method, as opposed to methide abstraction by borane (e.g. $B(C_6F_5)_3$), gives ion pairs that permute diastereotopic Cp methyl groups only by the ips pathway and avoids complications associated with deconvoluting the borane dissociation (dr pathway) (Scheme 1). Fewer solution dynamic studies have been reported for metallocenium ions paired with perfluoroarylborate counteranions, since they are more difficult to produce cleanly and are subject to more facile decomposition [2a]. Furthermore, these ion pairs are typically less soluble in non-polar media such as toluene than ones with methylborate counteranions, leading to samples forming oily clathrate-like residues if the concentration is too high ($[Zr] \gtrapprox 10$ mM).

A series of trityl borate salts (**[1-A]**) including $[CPh_3]^+\{C_6F_4$-1,2-$[B(C_6F_5)_2]_2(\mu\text{-}O(C_6F_5))\}^-$ (**[1-O(C_6F_5)]**), $[CPh_3]^+\{C_6F_4$-1,2-$[B(C_6F_5)_2]_2(\mu\text{-}OPh)\}^-$ (**[1-OPh]**), $[CPh_3]^+\{C_6F_4$-1,2-$[B(C_6F_5)_2]_2(\mu\text{-}OMe)\}^-$ (**[1-OMe]**), and $[CPh_3]^+[B(C_6F_5)_4]^-$ (**[1-B(C_6F_5)$_4$]**), were utilized to produce ion pairs of the general form $[Cp''_2ZrMe]^+[A]^-$, **[2-A]**, in arene solvents such as toluene or bromobenzene (Scheme 2). In all cases a slight excess of trityl salt was utilized to avoid unwanted dimeric $[(L_2MMe)_2(\mu\text{-}Me)]^+$ metallocenium fragments, which are readily identifiable by the upfield shifted resonance for the bridging methyl group in the ^1H NMR spectrum [16]. (Rate enhancements of anion symmetrization, potentially via $[Cp''_2Zr]^{2+}[A]^-_2$ species, were not observed in the presence of excess trityl borate salt.)

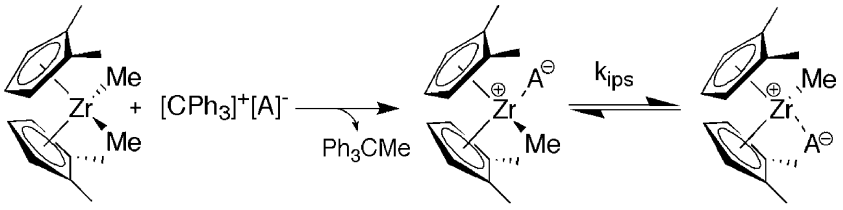

[1-A] **[2-A]**

A^- = {C_6F_4-1,2-[$B(C_6F_5)_2]_2(\mu$-$O(C_6F_5)$)}$^-$, **[N-O(C_6F_5)]**
A^- = {C_6F_4-1,2-[$B(C_6F_5)_2]_2(\mu$-OPh)}$^-$, **[N-OPh]**
A^- = {C_6F_4-1,2-[$B(C_6F_5)_2]_2(\mu$-OMe)}$^-$, **[N-OMe]**
A^- = $[B(C_6F_5)_4]^-$, **[N-B(C_6F_5)$_4$]**

Scheme 2.

Spectroscopic investigations were conducted on samples at concentrations between 2.5 and 10 mM in zirconium. The samples of **[2-A]** examined were found to be stable over several hours at room temperature and up to a week at low temperature (−40 °C). The decomposition products that resulted have not been identified but appear to be derived only from the cation [1,17], since the anions remain intact as monitored by ^{19}F NMR spectroscopy.

The rates and activation parameters for ion pair symmetrization were determined in toluene-d_8 unless stated otherwise using coalescence measurements [18], line broadening [18], 2D-EXSY [19], and 1D-DPFGSE-NOE [20]; data for the ion pairs studied are shown in Table 1. Rate data were determined over an average temperature range of 30 °C with typical data sets collected over a temperature range of −30 to −70 °C, except for **[2-O(C_6F_5)]** which exhibited observable exchange above room temperature. A broader range of temperature was restricted by increasing solvent viscosity at lower temperatures and by the coalescence point of the ion pairs in question at higher temperatures. Rate constants at various temperatures were not determined for the ion pair **[2-B(C_6F_5)$_4$]** since the instability of the ion pair and its poor solubility in toluene-d_8 precluded meaningful data collection. Finally, we tested the accuracy of our measurements by repeating the measurements made by Marks et al. for $[Cp''_2ZrCH_3]^+[H_3CB(C_6F_5)_3]^-$, which exhibited a positive $\Delta S^{\ddagger}$ of 13 ± 2 eu [3e], and those made by Brintzinger et al. on the *ansa* derivative $[Me_2Si(C_5H_4)_2ZrCH_3]^+[H_3CB(C_6F_5)_3]^-$, which exhibited a substantial negative $\Delta S^{\ddagger}$ of −19 ± 2 eu [5c]. In both cases we found that our results were the same, within experimental error, as those reported in the literature (see Table S-2, supporting information). A complete listing of collected rate constants can be found in the supporting information.

A combination of the dynamic NMR methods available were employed for each ion pair symmetization process and the results obtained for the compounds **[2-OPh]** and **[2-OMe]** are shown in Fig. 1, which displays overlaid Eyring plots for each of the methods used (line broadening, 2D-EXSY, and 1D-DPFGSE-NOE). The plots demonstrate the excellent agreement for each of the rate constants determined by each method. These results indicate that the methods are compatible and provide internal reproducibility and confidence in the data; use of several methods also allowed us to extend the temperature range of collectable rate data due to the increased sensitivity of 2D-EXSY and 1D-DPFGSE-NOE measurements at lower temperatures.

The activation parameters for ion pair symmetrization measured in this way for ion pairs **2** are comparable to those measured in other borate stabilized metallocenium ions [5c,12], although considerable variation in the $\Delta S^{\ddagger}$ values seems to be the norm in these systems. For example, Brintzinger et al. report values between −7.2 ± 5 and 24.4 ± 6 eu for $[B(C_6F_5)_4]^-$ partnered with various metallocenium ions [5c], while Marks et al. report values of 10 ± 1 eu for the $[Cp''_2ZrCH_3]^+$ salts of $[B(C_6F_4TBS)_4]^-$ (TBS = *tert*-butyldimethylsilyl) and $[B(C_6F_4TIPS)_4]^-$ (TIPS = triisopropylsilyl) [12c]. For ion pairs **2**, we observe slightly negative $\Delta S^{\ddagger}$ values ranging between −1 and −15 eu (Table 1). Brintzinger et al. have interpreted negative $\Delta S^{\ddagger}$ values as implicating

Table 1
Activation parameters for ion pair symmetrization in ion pairs **2**

Ion pair	$\Delta G^{\ddagger}_{298}$ (kcal mol^{-1})	$\Delta H^{\ddagger}$ (kcal mol^{-1})	$\Delta S^{\ddagger}$ (eu)	T_c (°C)	Methods
[2-O(C_6F_5)]	18.6 ± 1.7	16.2± 1.7	−8 ± 3	102 ± 1	T_c[a], LB(2)
[2-OPh]	13.1 ± 0.6	9.8 ± 0.4	−11 ± 2	−5 ± 1	T_c[a], LB(2), EXSY, DPFGSE-NOE
[2-OMe]	13.3 ± 0.8	8.8 ± 0.5	−15 ± 2	7 ± 1	T_c[a], LB, EXSY, DPFGSE-NOE
[2-B(C_6F_5)$_4$][b]	13 ± 3[c]			7 ± 3	T_c[a]

[a] T_c = coalescence measurement.
[b] 10% C_6D_5Br added for solubility.
[c] $\Delta G^{\ddagger}_{coal.}$.

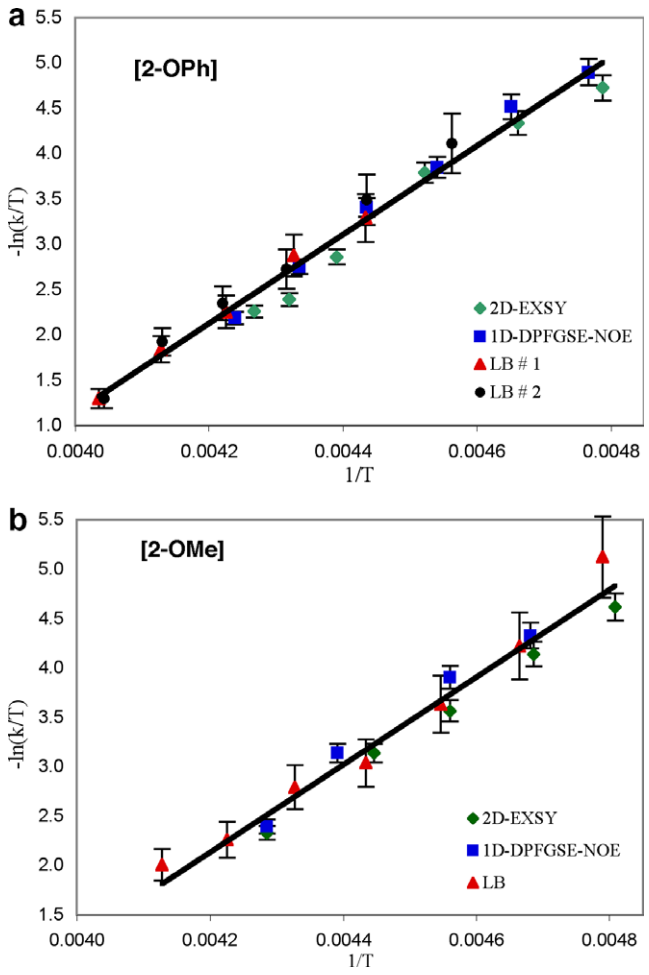

Fig. 1. Overlaid Eyring plots for ion pair symmetrization in **[2-OPh]** (a, top) and **[2-OMe]** (b, bottom) using line broadening, 2D-EXSY, and 1D-DPFGSE-NOE measurements.

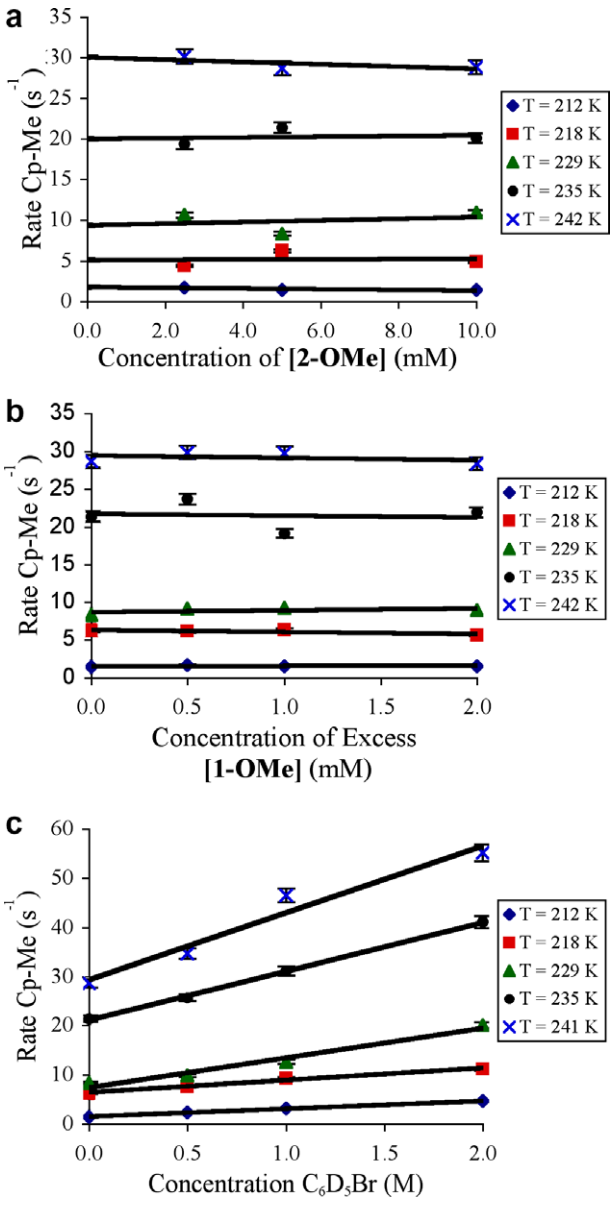

Fig. 2. Anion symmetrization rate constants in **[2-OMe]** as a function of (a) added **[1-OMe]**; (b) increasing concentration of **[2-OMe]**; (c) added C_6D_5Br.

the involvement of ion pair aggregates in the mechanism of ion pair symmetrization, and while there is substantial evidence that such aggregates exist in more ionized systems [12a,21] such as the borate stabilized metallocenium species discussed here, it is generally acknowledged that such aggregates do not play a significant role in the low concentration regimes we are operating in here [12a]. Consistent with this, the rate of ion pair symmetrization for **2-OMe** was independent of added trityl borate salt **1-OMe** (0.5–2 mM) or increasing metallocene concentration (2.5–10 mM) of **[2-OMe]** (Fig. 2a and b). The absence of anion symmetrization rate enhancements under these conditions suggests unimolecular exchange processes, which rules out a bimolecular (in metallocene) associative ion pair symmetrization mechanism.

This being said, the negative $\Delta S^{\ddagger}$ values in these and other systems, and indeed the wide variation in this parameter in comparable systems, requires some explanation. A two-step mechanism involving solvent displacement of the anion to form a solvent separated ion pair [22,23] (Scheme 3) is one possibility to account for the observations. Here, the displacement of the anion by a solvent molecule may assume associative or dissociative character depending on the size of the cation or the anion, and the nature of the cation/anion interactions. The picture presented assumes that symmetrization of the diastereotopic groups from the solvent separated ion pair is rapid compared to ion displacement. Consistent with this mechanism are observations of accelerated rates in more polar solvents equipped with donor groups. Marks et al. observed significantly enhanced rates of symmetrization in more polar solvents [3c] (along with more negative $\Delta S^{\ddagger}$ values), and we also observe this, as the observed rate of symmetrization for **2-OMe** increases as C_6D_5Br is added to the sample (increasing amounts of C_6D_5Br from 0 to 2.0 M, Fig. 2c).

In terms of $\Delta H^{\ddagger}$ values, those found for compounds **2** are similar to each other with the exception of **2-O(C_6F_5)**, which has an enthalpy of activation that is somewhat higher than

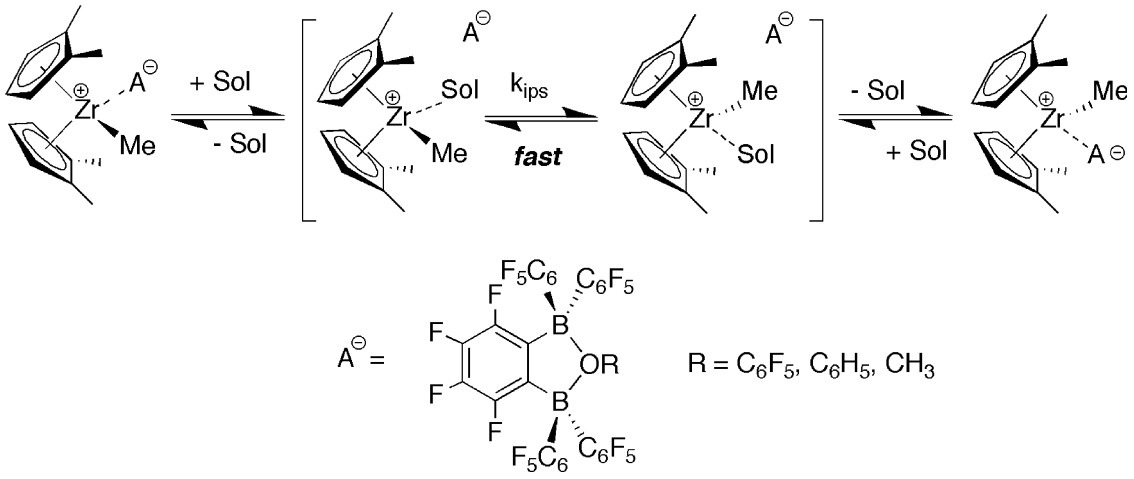

Scheme 3.

the others in the series. Values for $\Delta H^{\ddagger}$ in this range are usually associated with more coordinating anions, such as the methylborate anion $[MeB(C_6F_5)_3]^-$. The origin of this increase in the enthalpic barrier for this anion is not clear, but it may be due to stronger coordination of the anion via the $-OC_6F_5$ fluorines [24], which may be sterically accessible to the metallocenium fragment. ^1H, ^{19}F-1D-NOE difference NMR experiments [12a,25] were suggestive of such interactions, via detectable NOE enhancements of the Cp–*H*, Cp–*Me* and Zr–*Me* resonances upon irradiation of the *meta* and *para*-O(C_6F_5) fluorine's of the $\{C_6F_4$-1,2-$[B(C_6F_5)_2]_2(\mu$-O(C_6F_5))$\}^-$ anion, but firm conclusions regarding the nature of the cation/anion interaction were not derivable from these experiments. Unfortunately, all attempts to crystallize **2-O(C_6F_5)** met with failure.

3. Experimental

3.1. General considerations

All compounds were prepared and handled under air- and moisture-free conditions using vacuum line techniques or a glovebox. Toluene-d_8 was dried over sodium and distilled prior to use. Bromobenzene-d_5, dichloromethane-d_2 and dichloromethane were dried over CaH_2 and distilled prior to use. All other solvents were dried and purified by passing through activated alumina and Q5 columns. $[CPh_3]^+\{C_6F_4$-1,2-$[B(C_6F_5)_2]_2(\mu$-OMe)$\}^-$ $[CPh_3]^+\{C_6F_4$-1,2-$[B(C_6F_5)_2](\mu$-O(C_6F_5))$\}^-$ [13], and Cp''_2ZrMe_2 [26] were prepared from literature procedures. $[CPh_3]^+[B(C_6F_5)_4]^-$ was generously donated by Nova Chemicals Ltd. Elemental analyses were performed by the instrumentation lab at the University of Calgary. Routine ^1H NMR and line broadening experiments were carried out on either a Bruker DRX-400 or Bruker AMX2-300 spectrometer. ^1H NMR spectra were referenced relative to TMS at 0 ppm. ^{19}F NMR were referenced relative to external $CFCl_3$. All variable temperature experiments were calibrated with methanol or ethylene glycol [27]. 1D-DPFGSE NOE and 2D-EXSY NMR experiments were performed on a Bruker DRX-400 spectrometer equipped with a pulsed field gradient probe. All metallocene samples were prepared *in situ*.

3.2. Solution dynamic techniques

Coalescence measurements where used to determine $\Delta G^{\ddagger}_{coal.}$ from Eq. (1), where T_c is the temperature at coalescence and δ_v is the peak separation (in Hz) at the slow exchange limit

$$\Delta G^{\ddagger}_{coal.} = (1.912 \times 10^{-2}) T_c [9.972 + \log(T_c/\delta_v)] \quad (1)$$

In the case were $\Delta H^{\ddagger}$ and $\Delta S^{\ddagger}$ values were determined, $\Delta G^{\ddagger}_{coal.}$ was verified using Eq. (2)

$$\Delta G^{\ddagger}_{coal.} = \Delta H^{\ddagger} - T_c \Delta S^{\ddagger} \quad (2)$$

Peak widths at half height from variable temperature line broadening experiments [18] were determined using GNMR software [28]. Rate constants were evaluated from Eq. (3), where W^* is the peak width (in Hz) at half height of the exchanging system and W_0 is the peak width (in Hz) at half height in the absence of exchange (slow exchange limit)

$$k = \pi(W^* - W_0) \quad (3)$$

Quantitative analysis of variable temperature 2D-EXSY [19] data was performed by measuring peak volumes with AURALIA software [29]. Data with t_1 and t_2 dimensions of 256 and 1024 real points respectively, were collected using a relaxation delay (D1) 5 times the T_1 of the resonances in question for eight scans of each FID. Mixing times were chosen between 0.05 and 0.75 s at various temperatures such that the diagonal-to-cross peak ratio was approximately 4:1. t_1 and t_2 dimensions were zero-filled to 2048 and 2048 points respectively. Rate constants for an equally populated system were evaluated utilizing Eq. (4), where τ_m is the mixing time and $r = \sum$Int(diagonal)/$\sum$Int(cross).

$$k = (1/\tau_m) \ln[(r+1)/(r-1)] \quad (4)$$

Quantitative analysis of variable temperature 1D-DPFGSE NOE [20] data was performed by measuring peak intensities with Bruker 1D WINNMR software [30].

Typical spectra (8–12) were collected with mixing times between 0.025 and 1.50 s with a relaxation delay (D1) set to 5 times the T_1 of the resonances in question. Rate constants were determined from fitting of the integrated intensities to Eqs. (5) and (6) using iterative least squares fitting with an Excel spreadsheet. With an equally populated system, I_1 and I_2 are integrated intensities of excitation and chemical exchange peaks, respectively, I_0 is one-half of the integrated intensity of Me at time = 0, and R_1 and R_2 are residual relaxation coefficients:

$$I_1 = I_0(1 + e^{-2kt})(e^{(-R_1 t)}) \quad (5)$$

$$I_2 = I_0(1 + e^{-2kt})(e^{(-R_2 t)}) \quad (6)$$

3.3. Error analysis

For all kinetic experiments the estimated error values are reported after the rate constants. These values were established upon examination of potential sources of experimental error including temperature accuracy, integration accuracy, mass and concentration accuracy, NMR sensitivity, and sample purity. Propagation of errors has led to the total estimated error. This method is beneficial for determining error from potential systematic sources of error such as temperature calibration of the NMR probe. The key values utilized for these studies are as follows: temperature – 2.5% error, line broadening measurements – 8% error, 2D-EXSY measurements – 1% error, and 1D-DPFGSE-NOE measurements – 1% error. Errors reported for the energetic parameters ($\Delta G^{\ddagger}$, $\Delta H^{\ddagger}$, and $\Delta S^{\ddagger}$) were also determined through error propagation.

3.4. Synthesis of $[CPh_3]^+\{C_6F_4$-1,2-$[B(C_6F_5)_2]_2$-$(\mu$-OPh$)\}^-$

A solution of trityl phenoxide (0.030 g, 0.089 mol) in dichloromethane (5 mL) was added to the diborane C_6F_4-1,2-$\{B(C_6F_5)_2\}_2$ (0.075 g, 0.089 mol) and stirred overnight at room temperature. Orange crystals were formed upon layering this solution with hexanes (20 mL) and cooling to −40 °C. The product was isolated upon filtration and washed three times with cold hexanes, then dried under reduced pressure. (0.095 g, 76%). ^{1}H NMR (CD_2Cl_2): δ 7.09 (m, 9H, –C*Ph*$_3$), 6.73 (m, 6H, –C*Ph*$_3$). ^{19}F NMR (CD_2Cl_2): δ −130.1 (8F, *o-F*), −138.6 (2F, C_6F_4–), −159.9 (4F, *p-F*), −163.7 (2F, C_6F_4–), −166.5 (8F, *m-F*). Anal. Calc. for $C_{55}H_{20}B_2F_{24}O \cdot CH_2Cl_2$: C, 53.40; H, 1.76. Found: C, 53.56; H, 1.47.

3.5. General procedure for activation

Solutions of zirconocene ion pairs ([Zr] = 2.5–10 mM) were prepared by transferring, with a microliter syringe, stock solutions containing the dimethyl zirconocene complex, [Zr] = 32.51 mmol/L, to stock solutions containing the activator, c = 20–30 mmol/L, directly in an NMR tube. Deuterated solvent was added to a final volume of 0.4 mL. A 0.1 equivalency of activator was added in excess to prevent the formation of dimeric species (except for concentration studies). *Note:* Determinations of the T1 relaxation times for each exchanging signal were determined prior to the collection of anion symmetrization rate constants by the various methods outlined above.

3.5.1. $[Cp''_2ZrMe]^+\{C_6F_4$-1,2-$[B(C_6F_5)_2]_2(\mu$-O$(C_6F_5))\}^-$ ***([2-O(C_6F_5)])***

^{1}H NMR (toluene-d_8, 333 K): δ 5.87 (m, 2H, Cp–*H*), 5.71 (m, 2H, Cp–*H*), 5.58 (m, 2H, Cp–*H*), 1.89 (s, 6H, Cp–*Me*), 1.48 (s, 6H, Cp–*Me*), 0.14 (s, 3H, Zr–*Me*). T_c was determined to be 375.15 K, and δ_v was determined to be 165.4 Hz. Exchange rate constants were determined for the Cp–Me signals. Line broadening – [Zr] = 5.0 mM: line widths determined between 305.5 and 382.3 K, W_0 was determined below 280 K.

3.5.2. $[Cp''_2ZrMe]^+\{C_6F_4$-1,2-$[B(C_6F_5)_2]_2(\mu$-OPh$)\}^-$ ***([2-OPh])***

^{1}H NMR (toluene-d_8, 237 K): δ 5.82 (m, 2H, Cp–*H*), 5.71 (m, 2H, Cp–*H*), 5.42 (m, 2H, Cp–*H*), 1.94 (s, 6H, Cp–*Me*), 1.45 (s, 6H, Cp–*Me*), 0.20 (s, 3H, Zr–*Me*). T_c was determined to be 268.45 K, and δ_v was determined to be 207.7 Hz. Exchange rate constants were determined for the α-Cp–H and Cp–Me signals (mixing times τ_m given in parentheses). Line broadening – [Zr] = 2.5 mM and [Zr] = 5.0 mM: line widths determined between 221.6 and 250.9 K, W_0 determined below 216 K. 2D-EXSY – [Zr] = 5.0 mM: T = 211.1 K (0.400 s), 216.9 K (0.225 s), 223.6 K (0.075 s), T = 230.4 K (0.060 s), T = 234.2 K (0.050 s), T = 237.1 K (0.060 s). 1D-DPFGSE NOE – [Zr] = 2.5 mM: T = 212.0, 217.3, 222.7, 228.0, 233.4, 238.7 K.

3.5.3. $[Cp''_2ZrMe]^+\{C_6F_4$-1,2-$[B(C_6F_5)_2]_2(u$-OMe$)\}^-$ ***([2-OMe])***

^{1}H NMR (toluene-d_8, 227 K): δ 5.78 (m, 2H, Cp–*H*), 5.70 (m, 2H, Cp–*H*), 5.40 (m, 2H, Cp–*H*), 3.65 (s, 3H, μ-OMe), 1.93 (s, 6H, Cp–*Me*), 1.43 (s, 6H, Cp–*Me*), 0.25 (s, 3H, Zr–*Me*). T_c was determined to be 279.80 K, and δ_v was determined to be 221.2 Hz. Exchange rate constants were determined for the α-Cp–H and Cp–Me signals (mixing times τ_m given in parentheses). Line broadening – [Zr] = 10.0 mM: line widths determined between 211.0 and 245.2 K, W_0 determined at 205.3 K. 2D-EXSY – [Zr] = 6.6 mM: T = 210.1 K (0.350 s), T = 215.7 K (0.175 s), 221.7 K (0.125 s), 227.5 K (0.075 s), 236.1 K (0.050 s). 1D-DPFGSE NOE – [Zr] = 6.6 mM: T = 215.9, 221.7, 230.4, 236.1 K.

3.6. Additive concentration studies with the ion pair ***[2-OMe]***

(a) *Metallocene concentration*: Anion symmetrization rate constants, determined by 1D-DPFGSE NOE NMR spectroscopy, were obtained for the ion pair **[2-OMe]** at

the following concentrations [Zr] = 2.5, 5.0, 10.0 mM. T = 212.0, 218.4, 229.8, 235.5, 241.9 K.

(b) **[1-OMe]** *concentration*: Anion symmetrization rate constants, determined by 1D-DPFGSE NOE NMR spectroscopy, were obtained for the ion pair **[2-OMe]** in the presence of excess trityl salt **[1-OMe]** at the following concentrations: [Zr] = 5.0, 0.5, 1.0 and 2.0 mM excess [**1-OMe**]; T = 212.0, 218.4, 229.8, 235.5, 241.9 K.

(c) *C_6D_5Br concentration*: Anion symmetrization rate constants, determined by 1D-DPFGSE NOE NMR spectroscopy, were obtained for the ion pair **[2-OMe]** in the presence of C_6D_5Br in the following concentrations: [Zr] = 5.0, 0.5, 1.0, 2.0 mM C_6D_5Br; T = 212.0, 218.4, 229.8, 235.5, 241.9 K.

3.6.1. $[Cp''_2ZrMe]^+[B(C_6F_5)_4]^-$ ($[\mathbf{2\text{-}B(C_6F_5)_4}]$)

Addition of the metallocene solution to the activator solution was done at 195 K. The solution was slowly warmed in the NMR probe. ^{1}H NMR (90% toluene-d_8/10% C_6D_5Br, 230 K): δ 5.80 (m, 2H, Cp–*H*), 5.73 (m, 2H, Cp–*H*), 5.52 (m, 2H, Cp–*H*), 1.95 (s, 6H, Cp–*Me*), 1.49 (s, 6H, Cp–*Me*), 0.09 (s, 3H, Zr–*Me*). *Note:* Compound oils out over about 1 hour below 273 K and is not stable above room temperature. T_c was determined to be 279.92 K, and δ_v was taken as an average of all other determinations of δ_v, ~186 Hz.

Acknowledgements

Funding for this work came from the Natural Sciences and Engineering Research Council of Canada in the form of a Discovery Grant (to W.E.P.) and Postgraduate Fellowship support (to L.D.H.).

Appendix A. Supplementary material

Examples of each solution dynamic method, a listing of all rate data collected, and experimental for comparison studies to the ion pairs $[Cp''_2ZrMe]^+[MeB(C_6F_5)_3]^-$ and $[Me_2SiCp_2ZrMe]^+[MeB(C_6F_5)_3]^-$. Supplementary data associated with this article can be found, in the online version, at doi:10.1016/j.jorganchem.2007.05.023.

References

[1] (a) R.F. Jordan, Adv. Organomet. Chem. 32 (1991) 325;
(b) H.-H. Brintzinger, D. Fischer, R. Mülhaupt, B. Rieger, R.M. Waymouth, Angew. Chem., Int. Ed. Engl. 34 (1995) 1143;
(c) L. Resconi, L. Cavallo, A. Fait, F. Peimontesi, Chem. Rev. 100 (2000) 1253;
(d) G.W. Coates, Chem. Rev. 100 (2000) 1223;
(e) M. Bochmann, J. Chem. Soc., Dalton Trans. (1996) 255.
[2] (a) E.Y.-X. Chen, T.J. Marks, Chem. Rev. 100 (2000) 1391;
(b) A. Macchioni, Chem. Rev. 105 (2005) 2039;
(c) M. Bochmann, J. Organomet. Chem. 689 (2004) 3982.
[3] (a) M.V. Metz, D.J. Schwartz, C.L. Stern, T.J. Marks, Organometallics 21 (2002) 4159;
(b) M.-C. Chen, J.A. Roberts, T.J. Marks, J. Am. Chem. Soc. 126 (2004) 4605;
(c) C.L. Beswick, T.J. Marks, J. Am. Chem. Soc. 122 (2000) 10358;
(d) L. Li, C.L. Stern, T.J. Marks, Organometallics 19 (2000) 3332;
(e) C.L. Beswick, T.J. Marks, Organometallics 18 (1999) 2410;
(f) P.A. Deck, C.L. Beswick, T.J. Marks, J. Am. Chem. Soc. 120 (1998) 1772;
(g) L. Li, T.J. Marks, Organometallics 17 (1998) 3996;
(h) E.Y.-X. Chen, M.V. Metz, L. Li, C.L. Stern, T.J. Marks, J. Am. Chem. Soc. 120 (1998) 6287;
(i) Y.-X. Chen, C.L. Stern, T.J. Marks, J. Am. Chem. Soc. 119 (1997) 2582;
(j) P.A. Deck, T.J. Marks, J. Am. Chem. Soc. 117 (1995) 6128;
(k) X. Yang, C.L. Stern, T.J. Marks, J. Am. Chem. Soc. 116 (1994) 10015;
(l) X. Yang, C.L. Stern, T.J. Marks, J. Am. Chem. Soc. 113 (1991) 3623.
[4] (a) G. Erker, Dalton Trans. (2005) 1883;
(b) W.E. Piers, Adv. Organomet. Chem. 52 (2005) 1.
[5] (a) K. Bryliakov, D.E. Babushkin, E.P. Talsi, A.Z. Voskoboynikov, H. Gritzo, L. Schroeder, H.-R.H. Damrau, U. Weiser, F. Schaper, H.-H. Brintzinger, Organometallics 24 (2005) 894;
(b) F. Schaper, F. Geyer, H.-H. Brintzinger, Organometallics 21 (2002) 473;
(c) S. Beck, S. Lieber, F. Schaper, A. Geyer, H.-H. Brintzinger, J. Am. Chem. Soc. 123 (2001) 1483.
[6] (a) F. Song, S.J. Lancaster, R.D. Cannon, M. Schormann, S.M. Humphrey, C. Zuccaccia, A. Macchioni, M. Bochmann, Organometallics 24 (2005) 1315;
(b) F. Song, R.D. Cannon, M. Bochmann, J. Am. Chem. Soc. 125 (2003) 7641;
(c) S.J. Lancaster, A. Rodriguez, A. Lara-Sanchez, M.D. Hannant, D.A. Walker, D.L. Hughes, M. Bochmann, Organometallics 21 (2002) 451;
(d) A. Rodriguez-Delgado, M.D. Hannant, S.J. Lancaster, M. Bochmann, Macromol. Chem. Phys. 204 (2004) 334.
[7] (a) Z. Liu, E. Somsook, C.B. White, K.A. Rosaaen, C.R. Landis, J. Am. Chem. Soc. 123 (2001) 11193;
(b) C.R. Landis, K.A. Rosaaen, J. Uddin, J. Am. Chem. Soc. 124 (2002) 12062;
(c) C.R. Landis, K.A. Rosaaen, D.R. Sillars, J. Am. Chem. Soc. 125 (2003) 1710;
(d) D.R. Sillars, C.R. Landis, J. Am. Chem. Soc. 125 (2003) 9894.
[8] (a) A. Al-Humydi, J.C. Garrison, W.J. Youngs, S. Collins, Organometallics 24 (2005) 193;
(b) M. Mohammed, M. Nele, A. Al-Humydi, S. Xin, R.A. Stapleton, S. Collins, J. Am. Chem. Soc. 125 (2003) 7930.
[9] (a) V. Busico, V. Van Axel Castelli, P. Aprea, R. Cipullo, A. Segre, G. Talarico, M. Vacatello, J. Am. Chem. Soc. 125 (2003) 5451;
(b) V. Busico, R. Cipullo, W.P. Kretschmer, G. Talarico, M. Vacatello, V. Van Axel Castelli, Angew. Chem., Int. Ed. 41 (2002) 505.
[10] (a) J.C. Yoder, J.E. Bercaw, J. Am. Chem. Soc. 124 (2002) 2548;
(b) G.M. Wilmes, J.L. Polse, R.M. Waymouth, Macromolecules 35 (2002) 6766.
[11] (a) A. Correa, L. Cavallo, J. Am. Chem. Soc. 128 (2006) 10952;
(b) R. Fusco, L. Longo, F. Masi, F. Garbassi, Macromolecules 30 (1997) 7673;
(c) I.E. Nifant'ev, L.Y. Ustynyuk, D.N. Laikov, Organometallics 20 (2001) 5375;
(d) G. Lanza, I.L. Fragala', T.J. Marks, Organometallics 21 (2002) 5594;
(e) G. Lanza, I.L. Fragala', T.J. Marks, Organometallics 20 (2001) 4006;
(f) K. Vanka, T. Ziegler, Organometallics 20 (2001) 905;
(g) G. Lanza, I.L. Fragala', T.J. Marks, J. Am. Chem. Soc. 120 (1998) 8257;
(h) Z. Xu, K. Vanka, T. Firman, A. Michalak, E. Zurek, C. Zhu, T. Ziegler, Organometallics 21 (2002) 2444;
(i) Z. Xu, K. Vanka, T. Ziegler, Organometallics 23 (2004) 104;

(j) K. Vanka, Z. Xu, T. Ziegler, Can. J. Chem. 81 (2003) 1413;
(k) K. Vanka, Z. Xu, T. Ziegler, Organometallics 23 (2004) 2900;
(l) K. Vanka, M.S.W. Chan, C.C. Pye, T. Ziegler, Organometallics 19 (2000) 1841;
(m) M.S.W. Chan, K. Vanka, C.C. Pye, T. Ziegler, Organometallics 18 (1999) 4624.

[12] (a) C. Zuccaccia, N.G. Stahl, A. Macchioni, M.-C. Chen, J.A. Roberts, T.J. Marks, J. Am. Chem. Soc. 126 (2004) 1448;
(b) N.G. Stahl, C. Zuccaccia, T.R. Jensen, T.J. Marks, J. Am. Chem. Soc. 125 (2003) 5256;
(c) L. Jia, X. Yang, C.L. Stern, T.J. Marks, Organometallics 16 (1997) 842;
(d) L. Jia, X. Yang, A. Ishihara, T.J. Marks, Organometallics 14 (1995) 3135.

[13] V.C. Williams, G.J. Irvine, W.E. Piers, Z. Li, S. Collins, W. Clegg, M.R.J. Elsegood, T.B. Marder, Organometallics 19 (2000) 1619.

[14] V.C. Williams, W.E. Piers, W. Clegg, S. Collins, T.B. Marder, J. Am. Chem. Soc. 121 (1999) 3244.

[15] (a) J.C.W. Chien, W.-M. Tsai, M.D. Rausch, J. Am. Chem. Soc. 113 (1991) 8570;
(b) J.A. Ewen, M.J. Elder, Eur. Pat. Appl. 0,426,637, 1991.

[16] (a) K. Köhler, W.E. Piers, A.P. Jarvis, S. Xin, Y. Feng, A.M. Bravakis, S. Collins, W. Clegg, G.P.A. Yap, T.B. Marder, Organometallics 17 (1998) 3557;
(b) Y.-X. Chen, C.L. Stern, S. Yang, T.J. Marks, J. Am. Chem. Soc. 118 (1996) 12451;
(c) S. Beck, M.-H. Prosenc, H.-H. Brintzinger, R. Goretzki, N. Herfert, G. Fink, J. Mol. Catal. 111 (1996) 67;
(d) M. Bochmann, S.L. Lancaster, Angew. Chem., Int. Ed. Engl. 33 (1994) 1634;
(e) M. Bochmann, S.L. Lancaster, M.B. Hursthouse, K. Malik, Organometallics 13 (1994) 2235;
(f) M.P. Coles, R.F. Jordan, J. Am. Chem. Soc. 119 (1997) 8125.

[17] A. Bertuleit, C. Fritze, G. Erker, R. Frohlich, Organometallics 16 (1997) 2891.

[18] J. Sandström, Dynamic NMR Spectroscopy, Academic Press, Toronto, 1982.

[19] C.L. Perrin, T.J. Dwyer, Chem. Rev. 90 (1990) 935.

[20] (a) K. Stott, J. Keeler, Q.N. Van, A.J. Shaka, J. Mag. Res. 127 (1997) 302;
(b) K. Stott, J. Stonehouse, J. Keeler, T.-L. Hwang, A.J. Shaka, J. Am. Chem. Soc. 117 (1995) 4199;
(c) J. Stonehouse, P. Adell, J. Keeler, A.J. Shaka, J. Am. Chem. Soc. 116 (1994) 6037.

[21] S. Beck, A. Geyer, H.-H. Brintzinger, Chem. Commun. (1999) 2477.

[22] M.-H. Prosenc, H.-H. Brintzinger, J. Mol. Catal. 128 (1998) 41.

[23] M. Thornton-Pett, M. Bochmann, J. Am. Chem. Soc. (2001) 223.

[24] (a) J. Karl, G. Erker, R. Fröhlich, J. Am. Chem. Soc. 119 (1997) 11165;
(b) X. Yang, C.L. Stern, T.J. Marks, Angew. Chem., Int. Ed. Engl. 31 (1992) 1375;
(c) A.J. Mountford, D.L. Hughes, S.J. Lancaster, J. Chem. Soc., Chem. Commun. (2003) 2148.

[25] D. Neuhaus, M. Williamson, The Nuclear Overhauser Effect in Structural and Conformational Analysis, VCH Publishers, New York, 1989.

[26] G.M. Smith, Ph.D. Thesis, Northwestern University, 1985.

[27] C. Amman, P. Meier, A.E. Merbach, J. Mag. Res. 46 (1982) 319.

[28] P.H.M. Budzelaar, GNMR Version 3.6 for Windows, Oxford, 1995.

[29] P. Neidig, C. Fischer, Aurelia-Amix-Viewer Package for Bruker Suite, Version 3.0.1.

[30] 1D WINNMR software for Bruker NMR Suite; Version 6.0.